

COOLING EFFECT ENHANCEMENT IN MAGNETRON SPUTTERING SYSTEM

Jae-Sang BAEK and Youn J. KIM*

School of Mechanical Engineering,
Center for Advanced Plasma Surface Technology, Sungkyunkwan University,
300 Cheoncheon-dong, Suwon 440-746, Korea

* yjkim@skku.edu

ABSTRACT

Magnetron Sputtering system is a vacuum process used to deposit thin films on substrate for a wide variety of commercial and scientific purposes, such as making ultra-thin semiconductors, metal films, etc. It plays an important role in a coating system. In order to get the uniform deposition of material surface, high voltage and electric current are used in magnetron sputtering system. That energy is converted to heat, which must be removed by the appropriate cooling system. Otherwise, it may damage the target, the magnets, and the substrate as well. Therefore, in order to maintain the uniform deposition, the design of effective cooling system is important above all things. The main parameters affecting the cooling performance are the flow path of cooling water, inlet size and flow rate, etc. The flow characteristics of inside cooling system with various flow paths of cooling water and flow rates are investigated and results are graphically depicted.

NOMENCLATURE

p	pressure
\vec{v}	velocity
ρ	density
μ	dynamic viscosity
k_{eff}	thermal conductivity
τ	viscous term
A	ampere
T	temperature

INTRODUCTION

Magnetron sputtering method has been developed rapidly over the last decade to the point where it has become established as the process of choice for the deposition of a wide range of industrially important coatings. The driving force behind this development is the increasing demand for high-quality functional films in many diverse market sectors. In many cases, magnetron sputtered films now outperform films deposited by other physical vapour deposition (PVD) processes, and can offer the same functionality as much thicker films produced by other surface coating techniques.

In the basic sputtering process, a target (or cathode) plate is bombarded by energetic ions generated in glow discharge plasma, situated in front of the target as shown in Fig. 1. The bombardment process causes the removal of target atoms, which may then condense on a substrate as a thin film. Secondary electrons are also emitted from the target surface as a result of the ion bombardment, and these electrons play an important role in maintaining the plasma. The basic sputtering process has been known for many

years and many materials have been successfully deposited using this technique. However, the process is limited by low deposition rates, low ionisation efficiencies in the plasma, and high substrate heating effects (Arnell et al., 1999). These limitations have been overcome by the development of magnetron sputtering and, more recently, unbalanced magnetron sputtering. Magnetrons make use of the fact that a magnetic field configured parallel to the target surface can constrain secondary electron motion to the vicinity of the target. The magnets are arranged in such a way that one pole is positioned at the central axis of the target and the second pole is formed by a ring of magnets around the outer edge of the target. Trapping the electrons in this way substantially increases the probability of an ionising electron atom collision occurring. The increased ionisation efficiency of a magnetron results in a dense plasma in the target region. This, in turn, leads to increased ion bombardment of the target, giving higher sputtering rates and, therefore, higher deposition rates at the substrate.

In order to get higher deposition of material surface, high voltage and electric current are used in magnetron sputtering system. But most of the power input to the system appears finally as target heating. Such heating can become excessive local temperatures of 400°C have been reported (Kelly et al., 2000) and can lead to damage of the target, the magnets and the substrate as well.

Lake and Harding (1984) described a novel cathode target cooling technique which achieves good thermal contact between the target and backing plate while allowing differential thermal expansion to occur between the two materials. Also, Takatsuji et al. (1999) demonstrated the mechanism of the layered thin film growth by nanostructure analysis methods for sputter-deposited thin film and by thermal conductivity analysis for the cooling of the sputtering cathode through the experiment. However, there have been few reports on the

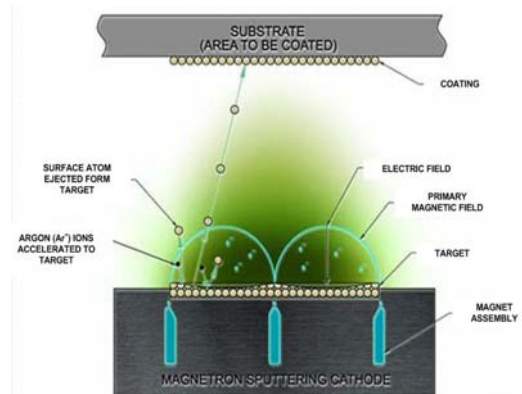


Figure 1: Schematic magnetron sputtering system (Angstrom science, 2006)

effect of target cooling in spite of important thing for deposition rate. This paper investigates the flow characteristics of inside cooling system and heat conduction between the target and working fluid with various flow paths of cooling water and flow rates to find the optimum condition for a magnetron sputtering system.

METHODOLOGY

Governing equations

In order to investigate the characteristics of cooling effects on the target by changing flow path and inlet velocity, the governing equations of continuity, momentum and energy can be expressed as follows:

continuity:

$$\nabla \cdot (\rho \vec{v}) = 0 \quad (1)$$

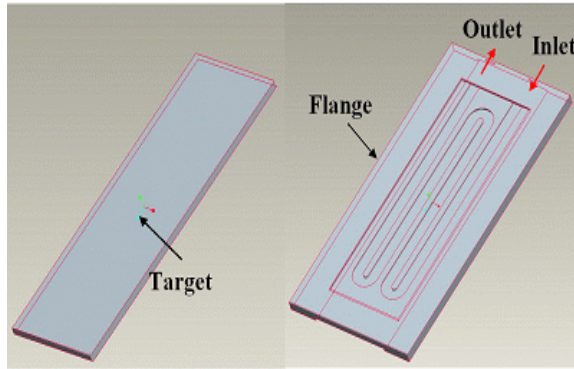
momentum:

$$\nabla \cdot (\rho \vec{v} \vec{v}) = -\nabla p + \nabla \cdot \tau F \quad (2)$$

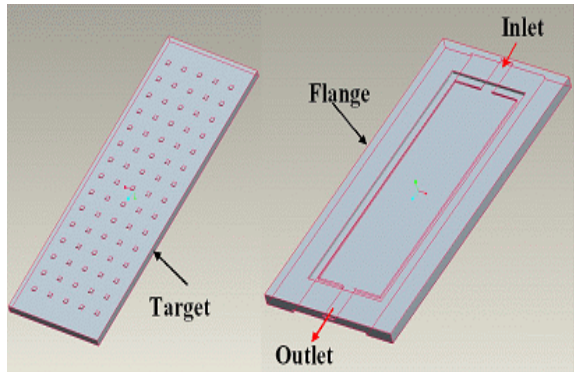
energy:

$$\nabla \cdot (\vec{v}(\rho E + p)) = \nabla \cdot (k_{eff} \nabla T) \quad (3)$$

where k_{eff} is the thermal conductivity and τ is the viscous term as follows:



(a) Type 1



(b) Type 2

Figure 2: Cooling channels of magnetron sputtering system

$$\tau = \mu[(\nabla \vec{v} + \nabla \vec{v}^T) - \frac{2}{3} \nabla \cdot \vec{v} I] \quad (4)$$

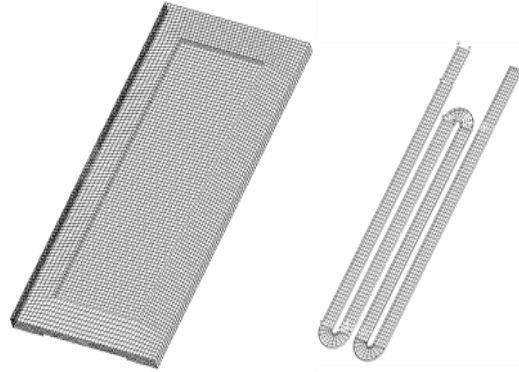
Here I is denoted as unit tensor.

Model and grid systems

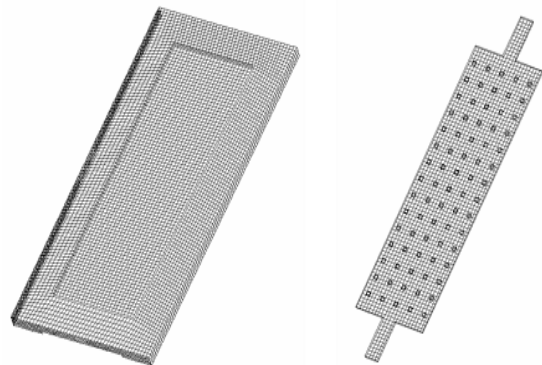
Schematic models of the magnetron sputtering system for numerical analysis with various cooling water paths are shown in Fig. 2. Type 1 shows the cooling system that used magnetron sputtering system under the present circumstances. Parts of system are constituted with titanium target (395 mm × 140 mm × 8mm) and backing plate (474 mm × 224 mm × 12mm) in which the carved flow path is carved. The shape of flow path is like alphabet “W”. Firstly, cooling water enters straight to the inside of cooling system, it turned three times and then came out to the same plane of the inlet. Shape of inlet and outlet port is rectangle and its cross-sectional area is 3 mm × 17 mm.

For the case of Type 2, it also has the same size of inlet and outlet ports as Type 1, but inlet and outlet ports are located in face to face plane. Also, there are 75 cooling fins. Each size is 5 mm × 5 mm × 2 mm in order to extend the heat exchange area. Shape of cooling water path has a rectangular parallelepiped which size (356 mm × 110 mm × 3 mm) is a little smaller than the target size. That shape also affects to extend the heat exchange area.

The computational grid system was formed by CFD pre-processor, GAMBIT. The configuration of grid system is depicted in Fig. 3. In order to investigate the cooling effect, three-dimensional grid systems were made of structured grids. We carried out tests from 200,000 to 600,000 elements for evaluating the numerical stability and convergence of the method. From these tests, the grid



(a) Type 1



(b) Type 2

Figure 3: Grid systems of the modelled cooling channels

Category	Content	Input
Working fluid	Flow	Steady, Turbulent
	Temperature	15 °C Liquid water
Target	Heat flux	100 kw/m ²
	Material	Titanium (k=7.44 w/m·k)
Backing plate	Material	SUS 304 (k=16.2 w/m·k)
Inlet	Velocity	0.25 m/s ~ 1 m/s
	Size	3 mm x 17 mm
wall	Condition	No slip

Table 1: Boundary conditions.

system composed of entirely from 450,000 to 500,000 elements was selected after those were proved that the results were stable. It represents in this problem the best compromise between the computational time and accuracy.

Numerical method and Boundary condition

Numerical analysis was executed with two different shapes of cooling water path and different values of inlet velocity, respectively. It is assumed that the working fluid flow is steady-state and turbulent ($Re=2530\sim5050$). In general, cooling water is evaporated in the part of cooling channel by influence of heat source, but we did not include two-phase (water-liquid and water-vapor) flows in our numerical simulation. Using a commercial CFD code, FLUENT, governing equations were discretized with FVM (Finite Volume Method) and solutions were obtained by SIMPLE (Semi-Implicit Method for Pressure-Linked Equations) algorithm (Versteeg et al., 1995). Also, in order to analysis turbulent flow, we used standard $k-\varepsilon$ model which is established by Launder and Spalding (1972). And no-slip wall boundary condition was applied on the all boundaries (White, 1995).

Target is the heat source of magnetron sputtering system. Value of heat flux is assumed 100 kW/m^2 to use the electric power density of magnetron sputtering system

(Jeong et al., 2003). Working fluid is used liquid water, and initial temperature is set to 15°C . In order to investigate the temperature distribution at the target surface, the velocity was changed from 0.25 m/s to 1 m/s . The boundary conditions required for the solution of numerical analysis are listed in Table 1.

RESULTS AND DISCUSSION

In this study, magnetron sputtering system was supplied with high electric current (10 A) in order to get higher deposition of material surface. We investigated the thermal distribution at the target surface with two different shapes of cooling water path and values of inlet velocity.

Figure 4 shows the temperature distribution of target surface and cooling channel for Type 1 with various values of the inlet flow velocity. Due to its 'W' shape of cooling water path and configuration, the working distance of cooling water is so long, and then the cooling efficiency of target is decreased. It is also seen from Fig. 4(a) that the value of maximum temperature deviation at the target surface is about 100°C between the inlet ($T=113^\circ\text{C}$) and outlet portions ($T=215^\circ\text{C}$) for $V_{in}=0.5\text{ m/s}$. Especially, temperature of the right side of target is 405°C . It appears that cooling does not arise at that section. Such an uneven temperature distribution may be resulted in the lower deposition rate. As shown in Fig. 4(b), temperature is getting higher gradually moved from inlet ($T=15^\circ\text{C}$) to outlet ($T=90^\circ\text{C}$), and the conduction is increased by low velocity in cooling channel. This can be deduced that the cooling efficiency of system is low to cooling all over the target.

The temperature deviation of target surface is changed by increment of inlet velocity. As shown in Fig. 4(c), the right side of target is still maintained high temperature ($T=330\sim380^\circ\text{C}$). Also, the temperature gap of cooling channel between the inlet and outlet is smaller as the inlet

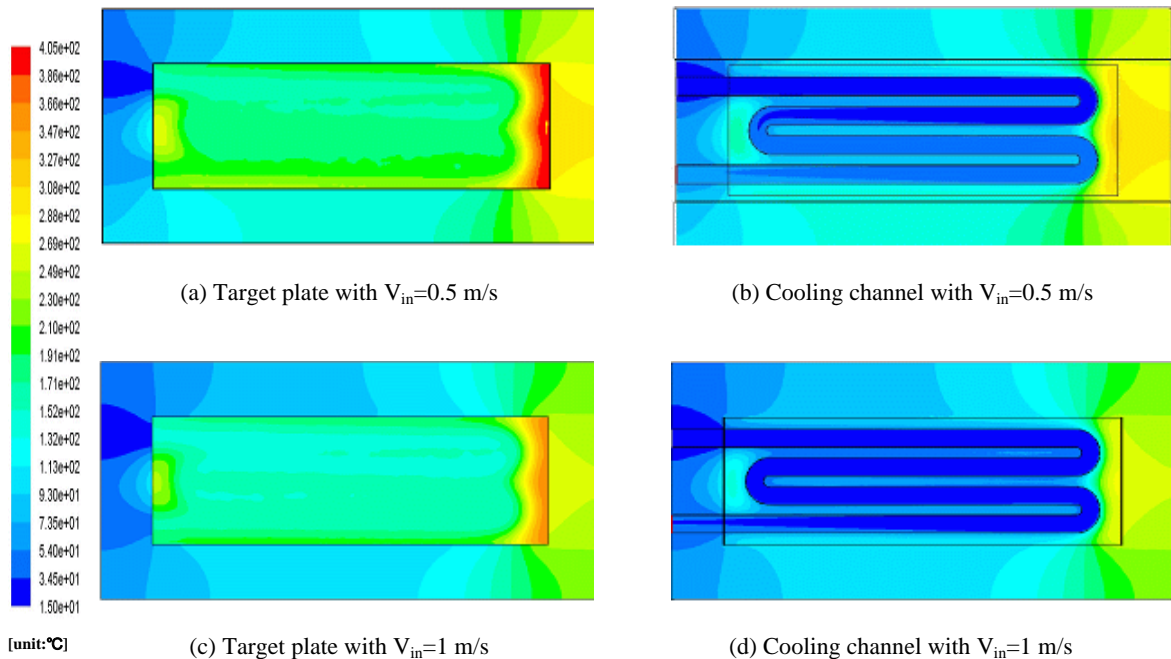


Figure 4: Temperature distributions of Type 1 with two different values of the inlet flow velocity

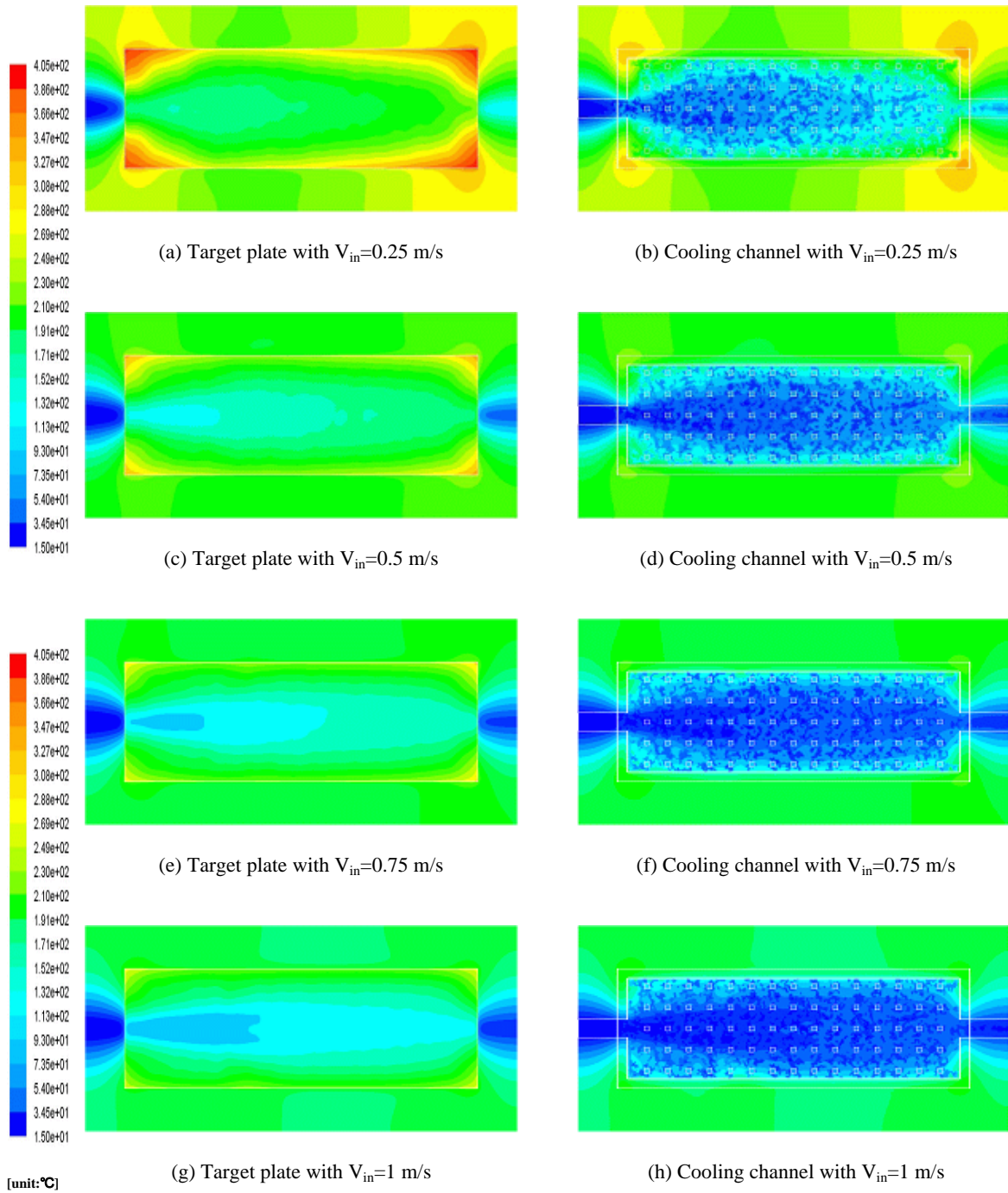


Figure 5: Temperature distributions of Type 2 with various values of the inlet flow velocity

velocity increases. In hence, increment of inlet velocity causes the decrease of total temperature at target surface except the right side of target and the temperature of working fluid maintains a little change compared with initial condition (i.e., 15°C).

In order to improve the performance of Type 1, inlet and outlet ports are located in face to face plane for decreasing the temperature at the right side of target and the shape of cooling channel is changed like a rectangular parallelepiped which size is a little smaller than the target size. Also, there are 75 cooling fins that each size is 5 mm × 5 mm × 2 mm in order to extend the heat transfer area.

As shown in Fig. 5(a), the highest value of temperature (386°C) is located near the corner of target and the

minimum temperature (130°C) is near the part of inlet port. The gap of temperature deviation at the target surface is shown very high, which will be resulted in the poor deposition rate and the quality of deposition. It is also seen that the working fluid is evaporated near the corner of target owing to the lack of inlet flux. It can be deduced by the value of temperature (190°C) from the result of Fig. 5(b).

It is seen from Fig. 5(c) that the temperature value near the corner is reduced to 171°C compared with Fig. 5(a) and the temperature distribution represents more uniform than Type 1. However, Type 2 has abrupt extension and reduction at the connection part between inlet, outlet ports

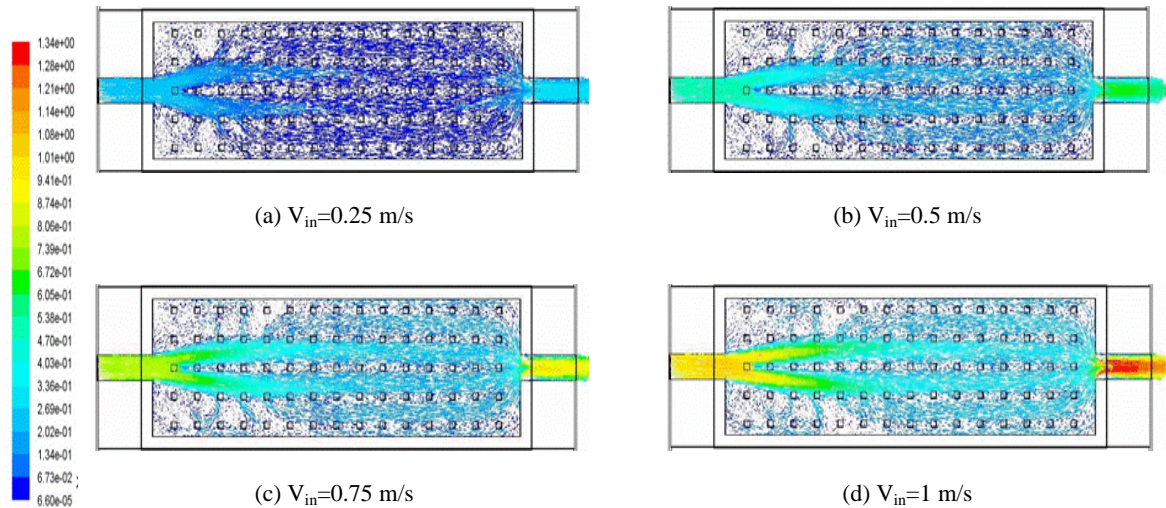


Figure 6: Velocity distributions of Type 2 with various values of the inlet flow velocity

and flow path. It creates dead spaces in which the cooling water is stagnating at the corner of flow path. Because of a dead space, temperature value is more than 100°C by heat source, and a small amount of working fluid is evaporated at the dead space. In hence, the local temperature shows extremely high value near the corner of target. The reason is that the value of thermal conductivity by water-vapor ($k_{\text{eff}}=0.02$ W/m-K) is smaller about 30 times than that of the water-liquid ($k_{\text{eff}}=0.6$ W/m-K).

As the inlet velocity is increased, total temperature and temperature of near the target corner are decreased. As shown in Fig. 5(e~h), however, the excessive cooling area is represented owing to the increment of working fluid flux, which is affected the uniform temperature distribution.

Figure 6 depicts the velocity distribution of Type 2 with various values of inlet flow velocity. It is seen that the eddy occurs at the corner of flow path through abrupt extension and reduction at the connection part between inlet, outlet ports and flow path.

CONCLUSIONS

Cooling effect enhancement in magnetron sputtering system was investigated with two different shapes of cooling water path and various value of inlet velocity. The following conclusions are obtained:

- 1) As the inlet velocity is increased, the total temperature at the target surface is decreased. But the value of temperature at the end of target is shown still high about 330~380°C, because there is no cooling water path under the end of target.
- 2) Cooling water path of Type 2 has the cooling fins of which bring about the extension of heat exchange area for enhancement of heat conduction efficiency. As a result, the value of temperature is represented 150~200°C. The temperature deviation of target surface is more uniform than Type 1 which used the cooling system under the present circumstances.
- 3) In the case of Type 2, the model has abrupt extension and reduction at the connection part between inlet, outlet ports and flow path. It makes dead space in which the cooling water stagnates at the corner of flow path.

It is needed to perform an in-depth study about optimal design of cooling system in magnetron sputtering system.

ACKNOWLEDGEMENT

The authors are grateful for the financial support provided by the Center of Excellency Program of the Korea Science and Engineering Foundation and Ministry of Science and Technology (Grant No. R11-2000-086-0000-0) through the Center for Advanced Plasma Surface Technology (CAPST) at the Sungkyunkwan University.

REFERENCES

- Angstrom science, (2006), Sputtering technology, <http://www.angstromsciences.com>.
- ARNELL, R. D., KELLY, P. J., (1999), "Recent advances in magnetron sputtering", Surface and Coating Technology, Vol. 112, pp. 170 – 176.
- JEONG, J. I., JUNG, W. C., IM, T. G., JUN, J. H., (2003), "Manufacturing and characterization of high rate magnetron sputtering source", RIST, Vol. 17(1), pp. 20-28.
- KELLY, P. J., ARNELL, R. D., (2000), "Magnetron sputtering a review of recent developments and applications", Vacuum, Vol. 56, pp. 159 – 172.
- LAKE, M. R., HARDING, G. L., (1984), "Cathode cooling apparatus for a planar magnetron sputtering system", Journal of Vacuum Science & Technology, A2(3), pp. 1391-1393.
- LAUNDER, B. E., SPALDING, D. B., (1972), Lectures in Mathematical Models of Turbulence, Academic Press, London.
- TAKATSUJI, H., TSUJI, S., KURODA, K., SAKA, H., (1999), "The influence of cooling water flowing in the sputtering target on aluminum based thin film nanostructure deposited on glass substrates," Thin Solid Films, Vol. 343-344, pp. 465-468.
- VERSTEEG, H. K., MALALASEKERA, M., (1995), An Introduction to Computational Fluid Dynamics the Finite Volume Method, John Wiley & Sons, New York.
- WHITE, F. M., (1995), Fluid Mechanics, 3rd Ed, McGraw-Hill, Singapore.